A&A 544, A19 (2012)
DOI: 10.1051/0004-6361/201219674

Astronomy & Astrophysics

Accurate rotational rest-frequencies of CH_2NH at submillimetre wavelengths⋆

L. Dore[1], L. Bizzocchi[2], and C. Degli Esposti[1]

[1] Dipartimento di Chimica "G. Ciamician", Università di Bologna, via F. Selmi 2, 40126 Bologna, Italy
e-mail: [claudio.degliesposti;luca.dore]@unibo.it
[2] Centro de Astronomia e Astrofísica, Observaório Astronómico de Lisboa, Tapada da Ajuda, 1349-018 Lisboa, Portugal
e-mail: bizzocchi@oal.ul.pt

Received 24 May 2012 / Accepted 16 June 2012

ABSTRACT

Context. Methanimine (CH_2NH) has been detected in different astronomical sources, both galactic (as in several "hot cores", the circumstellar enevolope IRC+10216, and the L183 pre-stellar core) and extragalactic, and is considered a pre-biotic interstellar molecule. Its ground-state rotational spectrum has been studied in the laboratory up to 172 GHz, well below the spectral ranges covered by *Herschel*/HIFI and the ALMA bands 9 and 10.

Aims. In this laboratory study, we extend into the submillimetre-wave region the detection of the rotational spectrum of CH_2NH in its vibrational ground state.

Methods. The investigation was carried out using a source-modulation microwave spectrometer equipped with a cell coupled to a pyrolysis apparatus working at 1150 °C. The spectrum was recorded in the frequency range 329–629 GHz, with the detection of 58 transitions.

Results. The newly measured transition frequencies, along with those available from previous microwave studies, allow us to determine fairly accurate rotational constants of CH_2NH and the complete sets of quartic and sextic centrifugal distortion constants, in addition to two octic constants. Several transitions have an hyperfine structure due to the ^{14}N nucleus, which was accounted for in the analysis.

Conclusions. The determined spectroscopic constants make it possible to build a list of very accurate rest-frequencies for astrophysical purposes in the THz region with 1σ uncertainties lower than 0.01 km s^{-1} in radial equivalent velocity.

Key words. molecular data – methods: laboratory – techniques: spectroscopic – radio lines: ISM

1. Introduction

The simplest molecule containing a carbon–nitrogen double bond is methanimine (CH_2NH), which is also called methylenimine or formaldimine. It was detected for the first time in the molecular cloud Sgr B2 (Godfrey et al. 1973) towards the Galactic centre, although it is present there in low abundance (Turner 1991). CH_2NH is a reactive species, therefore unstable in the terrestrial environment, which may be considered as a pre-biotic interstellar molecule. Danger et al. (2011) prove that, by warming ice analogues in astrophysical-like conditions, methanimine participates in the Strecker synthesis to form aminoacetonitrile (NH_2CH_2CN; recently detected in Sgr B2(N) by Belloche et al. 2008), which is a possible precursor of glycine, the simplest amino acid.

In reality, CH_2NH has been found in several "hot cores" associated with massive star-forming regions (Dickens et al. 1997; White et al. 2003; Qin et al. 2010), where it is more abundant than in dark clouds because of its release to the gas phase from the heated grain mantles (Dickens et al. 1997). However, wether this partially saturated species is formed in the gas phase or on the dust grains has not been clearly established, as outlined by Turner et al. (1999) in their comparison of the observations of CH_2NH in one translucent molecular cloud with those in the L183 pre-stellar core. As far as circumstellar envelopes are concerned, discussing their recent detection of methanimine in the carbon-rich IRC+10216, Tenenbaum et al. (2010) assume a gas-phase formation, by the association of CH with NH_3, because CH_2NH is present in the outer envelope. In addition, the molecule was not detected by Schilke et al. (2001) in their submillimetre survey of the Orion KL hot core (IRc2); this confirmed previous findings (Dickens et al. 1997), suggesting that the CH_2NH emission observed towards Orion KL is associated with the "compact ridge", where lower temperature and intermediate density favour radiative association.

It is noteworthy that methanimine is one of the more than 50 molecules identified in extragalactic environments: it has been detected in the ultraluminous infrared galaxy Arp 220 (Salter et al. 2008), and tentatively in the starburst galaxy NGC 253 (Martín et al. 2006). Furthermore, the rotational 4-mm-rest-frame absorption line of CH_2NH was identified in the spectral line survey of a high-z molecular absorber, located at $z = 0.89$ in front of the quasar PKS 1830-211 (Muller et al. 2011). Finally, there is the hypothesis that CH_2NH is present in the atmosphere of Titan, where it might have been formed either from NH and CH_3 (Redondoa et al. 2006), by ion-chemistry

⋆ Table 1 is only available at the CDS via anonymous ftp to cdsarc.u-strasbg.fr (130.79.128.5) or via http://cdsarc.u-strasbg.fr/viz-bin/qcat?J/A+A/544/A19

(Vuitton et al. 2007), or via the N(^{2}D)+CH_4 reaction (Balucani et al. 2009).

Methanimine is a light molecule and its rotational spectrum shows increasing intensity and spectral density with frequency at submillimetre wavelengths. At the typical kinetic temperatures of the molecular gas in high-mass star-forming regions (50–200 K, see e.g., Dickens et al. 1997), many strong transitions of CH_2NH fall at frequencies higher than 400 GHz. Chemically rich regions will soon be the target of ALMA observations in this wavelength regime (bands 8 and 9, which will both be available in the forthcoming cycle 1), and are already being extensively surveyed by *Herschel*/HIFI (e.g., the HEXOS key programme, Bergin et al. 2010). With their improved sensitivity, high resolution, and the wideband coverage, these telescopes are expected to deliver a wealth of spectral data, hence the availability of submillimetre rest-frequencies with small uncertainties is crucial to unravel the chemical complexity and infer, from the observational data, the source physical parameters.

The laboratory rotational spectrum of methanimine was first recorded in the gas phase by Johnson & Lovas (1972) up to 123 GHz. In addition to the main species, several isotopologues ($H_2^{13}CNH$, $H_2C^{15}NH$, H_2CND, D_2CNH, and D_2CND) were later detected by microwave spectroscopy (Pearson & Lovas 1977) in order to determine the molecular structure of CH_2NH. Recently, several transitions falling in the range of 64–172 GHz were recorded in the laboratory study of Dore et al. (2010): the main focus was to study the magnetic hyperfine structure due to the interactions of ^{14}N and the three ^{1}H nuclear spins, which could be resolved by means of the Lamb-dip spectroscopy (Costain 1969; Winton & Gordy 1970).

The present laboratory investigation was undertaken to extend rotational frequency measurements of CH_2NH to submillimetre wavelengths, and makes it possible to build a list of very accurate rest-frequencies for astrophysical purposes in the THz region with 1σ uncertainties smaller than 0.01 km s^{-1} in radial equivalent velocity.

2. Experimental

Methanimine was produced by pyrolysis with the same apparatus employed in this laboratory to produce other molecules of astrophysical interest, such as HC_5N (Yamada et al. 2004), HC_7N (Bizzocchi & Degli Esposti 2004), and C_3O (Bizzocchi et al. 2008). The precursor used was ethylenediamine ($NH_2CH_2CH_2NH_2$; Hamada et al. 1984), which was heated to 1150 °C while flowing through a quartz tube (50 cm long and 1 cm in diameter) inserted in a 30 cm long cylindrical furnace. The quartz tube was connected to the gas inlet of the double-pass absorption cell, a glass tube 3 m long and 10 cm in diameter equipped with a wire grid polarizer and a roof mirror (Dore et al. 1999), through which the pyrolysis products were continuously pumped. The very effective production and the strong signals of methanimine allowed us to use a low flow in the reactor in order to record the spectra with a pressure in the cell no higher than 10 mTorr (=1.33 Pa).

Measurements were carried out in the frequency range of 329–629 GHz, by employing phase-locked Gunn oscillators (Radiometer Physics GmbH, J. E. Carlstrom Co) as primary radiation source working in the range of 75–115 GHz, and power at higher frequencies was obtained using harmonic multiplication. Two phase-lock loops allowed the stabilization of the Gunn oscillator with respect to a frequency synthesizer, which was driven by a 5-MHz rubidium frequency standard. The frequency modulation of the radiation was obtained by a sine-wave (at 6 kHz or 1.666 kHz for Lamb-dip measurements) modulating the reference signal of the wide-band Gunn synchronizer; the signal, detected by a liquid-helium-cooled InSb hot electron bolometer (QMC Instr. Ltd. type QFI/2), was demodulated at 2-*f* by a lock-in amplifier.

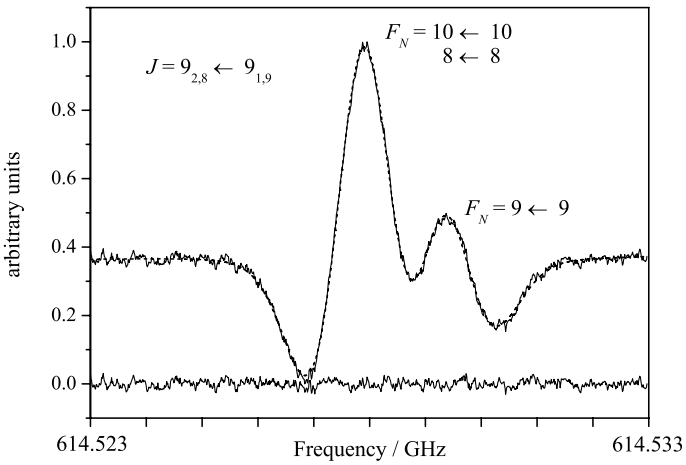

Fig. 1. Hyperfine doublet of the $J = 9_{2,8} \leftarrow 9_{1,9}$ rotational transition of CH_2NH; total integration time 310 s at 194 kHz/s with time constant of 10 ms. The spectral profile has been fit to a sum of three hyperfine components; fit residuals are shown at the bottom of the plot.

3. Analysis

CH_2NH is a near prolate ($\kappa = -0.937$) planar asymmetric rotor, where all the nuclei lie in the *ab* plane and the C–N bond is almost aligned with the *a* principal axis, thus the dipole moment has components along the *a* and *b* axes[1], and *a*-type and *b*-type transitions occur in its rotational spectrum. The newly observed transitions are listed in Table 1: there are R ($\Delta J = +1$) and Q ($\Delta J = 0$) *a*-type lines and R, Q, and P ($\Delta J = -1$) *b*-type lines. Some of them are partially split by the electric quadrupole coupling of the ^{14}N nucleus: the three $\Delta F = \Delta J$ hyperfine components either overlap or one is more or less partially resolved from the other two. For transitions appearing as a main blended peak, possibly with a shoulder, the unperturbed line frequency was recovered by a line shape analysis (Dore 2003) of the spectral profile, which is modelled as a sum of hyperfine components with their frequency shift and intensity fixed at the values accurately predicted using the hyperfine constants known from our previous work (Dore et al. 2010). In addition, for the transitions appearing as a doublet, the two frequencies were obtained by a line shape analysis, as is shown in Fig. 1.

The measured line frequencies fall in the submillimetre-wave region and allow us to extend the centrifugal analysis carried out in Dore et al. (2010). Present and previous hyperfine data[2] were fitted together, employing Pickett's SPFIT fitting program (Pickett 1991), to an asymmetric rotor Hamiltonian using Watsons S-reduced I^r representation (Watson 1977). The rotational constants, as well as the ^{14}N hyperfine constants, were

[1] $\mu_a = 1.3396$ D and $\mu_b = 1.4461$ D (Allegrini et al. 1979).

[2] The hf components of the $5_{1,4} \leftarrow 5_{1,5}$ transition, reported by Johnson & Lovas (1972), were measured again by Lamb-dip spectroscopy and two of them were split by magnetic interactions due to the three protons. Frequencies in MHz for the $F'_N \leftarrow F_N$ components are: $4 \leftarrow 4$: 79 280.1688, 79 280.1970; $6 \leftarrow 6$: 79 280.6682; and $5 \leftarrow 5$: 79 282.7901, 79 282.8120.

Table 2. Spectroscopic constants of CH_2NH.

	Experiment		
Constants	This work[a]	Ref.[1,b]	Ref.[2,b]
Rotational/MHz			
A_0	196 210.87642(51)	196 210.87559(57)	196 210.938(12)
B_0	34 641.699332(93)	34 641.69932(15)	34 641.7112(21)
C_0	29 351.496908(85)	29 351.49688(10)	29 351.5077(19)
Quartic centrifugal distortion/kHz			
D_J	56.00357(53)	56.0021(56)	55.961(23)
D_{JK}	598.6807(54)	598.639(83)	597.94(36)
D_K	6383.419(38)	6383.47(20)	6384.9(10)
d_1	–9.972737(59)	–9.97250(57)	–9.9690(21)
d_2	–2.007853(34)	–2.00805(26)	–2.00717(30)
Sextic centrifugal distortion/Hz			
H_J	0.01676(55)	0.[c]	–0.038(30)
H_{JK}	2.604(12)	2.32(12)	0.99(78)
H_{KJ}	6.118(75)	0.[c]	7.9(23)
H_K	877.0(11)	931.(16)	859.5(66)
h_1	0.032156(91)	0.0288(15)	0.0258(36)
h_2	0.032351(62)	0.0336(15)	0.03031(90)
h_3	0.009203(47)	0.00830(41)	0.00870(10)
Octic centrifugal distortion/mHz			
L_K	–159.8(49)	–	
l_3	$-0.558(41) \times 10^{-3}$	–	
N quadrupole coupling/MHz			
χ_{aa}	–0.9147(17)	–0.9148(12)	
$\chi_{bb} - \chi_{cc}$	–6.2478(20)	–6.2477(17)	
N spin-rotation/kHz			
C_{aa}	52.89(84)	52.73(64)	
C_{bb}	9.38(28)	9.45(22)	
C_{cc}	0.68(26)	0.66(20)	

Notes. [(a)] The errors reported in parentheses are in units of the last quoted digits, and standard errors of parameters can be obtained by multiplying by 0.971 (see $\sigma_{\rm fit}$ in Table 1). [(b)] Standard errors are reported in parentheses in units of the last quoted digits. [(c)] Fixed parameter in the fit.

References. [(1)] Dore et al. (2010); [(2)] Halonen & Duxbury (1985).

refined, and the complete sets of quartic and sextic distortion constants plus two octic ones were determined; all of them are reported in Table 2, where we compare with previous determinations by millimetre-wave (Dore et al. 2010) and IR (Halonen & Duxbury 1985) spectroscopy.

4. Discussion

This paper extends the laboratory study of the rotational spectrum of methanimine into the submillimetre-wave region (329–629 GHz). Several different types of transitions were recorded: for the *a*-type spectrum, the complete *K*-structure of the $J = 9 \leftarrow 8$ transition, the three lines $J = 10_{0,10} \leftarrow 9_{0,9}$, $10_{1,10} \leftarrow 9_{1,9}$, and $11_{0,11} \leftarrow 10_{0,10}$, and three transitions ($J = 24$, 25, and 27) of the *Q* band with $K_a = 3$; the *b*-type spectrum is very sparse, and very informative, therefore $\Delta J = 0, \pm 1$ transitions were observed, sampling states with the rotational quantum number *J* ranging from 1 to 36, and its projection K_a from 0 to 9.

These measured rotational frequencies, added to the variety of transitions previously measured in the millimetre-wave region, allowed us to determine rotational and centrifugal distortion constants with an accuracy higher than previously obtained, by almost an order of magnitude for the quartic and sextic distortion constants; in addition, two octic constants were determined. Transition frequencies predicted using these high-precision spectroscopic constants have uncertainties on average one order of magnitude smaller than predictions obtained with previous constants.

As an example of the small uncertainty attainable in the prediction of rest-frequencies, Table 3 reports a portion of the catalogue file obtained by running Pickett's SPCAT program (Pickett 1991) (with correlations between the spectroscopic constants considered), where predictions along with their 1σ uncertainties are listed for the 30 strongest transitions at 50 K in the ALMA band 10 (780–970 GHz). The frequency precision is of the order of a few parts in 10^9 (1 part in 10^9 corresponds to to $0.0003\,{\rm km\,s^{-1}}$ in radial velocity), and the lowest uncertainties are for transition frequencies with a relatively small centrifugal-distortion contribution. It is obvious that the predicted uncertainties are model-dependent (in addition to the predicted transition frequencies), in the sense that additional centrifugal terms, indeterminable with present data, can cause these to increase. However, the spectroscopic constants presently determined from measurements up to 629 GHz should allow a fairly accurate prediction of the rotational spectrum of methanimine at higher frequency, particularly for *b*-type transitions with small centrifugal contributions. Figure 2 shows the rotational spectrum up to 1 THz computed at 50 K, where it is apparent that at this temperature the strongest transitions of CH_2NH lie in the ALMA bands 9 and 10, and the *Herschel*/HIFI bands 1–3.

Table 3. Calculated hyperfine frequencies[a] of CH_2NH in the ALMA band 10 (780−970 GHz).

$J'_{K_a,K_c} \leftarrow J_{K_a,K_c}$	$F'_N \leftarrow F_N$	Calculated (MHz)	Uncertainty (kHz)	Line Strength
$12_{1,12} \leftarrow 11_{0,11}$	12 ← 11	781 525.5867	2.3	8.7205
	13 ← 12	781 526.0067	2.3	9.4840
	11 ← 10	781 526.0413	2.3	8.0179
$10_{3,7} \leftarrow 10_{2,8}$	10 ← 10	781 609.3661	2.1	5.3951
	11 ← 11	781 609.8559	2.2	5.9681
	9 ← 9	781 609.8777	2.1	4.9216
$5_{2,4} \leftarrow 4_{1,3}$	5 ← 4	785 938.0195	1.7	2.0412
	6 ← 5	785 939.0229	1.9	2.5128
	4 ← 3	785 939.2252	1.7	1.6537
$13_{1,13} \leftarrow 12_{1,12}$	13 ← 12	788 275.6000	2.4	12.830
	12 ← 11	788 275.6309	2.4	11.874
	14 ← 13	788 275.6413	2.4	13.863
$12_{1,11} \leftarrow 11_{1,10}$	12 ← 11	788 333.8715	2.2	11.806
	13 ← 12	788 333.9522	2.3	12.840
	11 ← 10	788 333.9529	2.2	10.855
$12_{2,10} \leftarrow 11_{2,9}$	11 ← 10	790 665.5597	2.3	10.657
	13 ← 12	790 665.5756	2.3	12.605
	12 ← 11	790 665.6397	2.3	11.591
$9_{3,6} \leftarrow 9_{2,7}$	9 ← 9	793 364.9838	2.0	4.7057
	10 ← 10	793 365.4079	2.1	5.2654
	8 ← 8	793 365.4185	2.1	4.2524
$13_{0,13} \leftarrow 12_{0,12}$	13 ← 12	796 740.0951	2.5	12.856
	12 ← 11	796 740.1984	2.5	11.898
	14 ← 13	796 740.2006	2.5	13.891
$8_{3,5} \leftarrow 8_{2,6}$	8 ← 8	802 589.0836	1.9	4.0462
	7 ← 7	802 589.4253	2.0	3.6141
	9 ← 9	802 589.4293	2.0	4.5931
$7_{3,4} \leftarrow 7_{2,5}$	7 ← 7	809 439.6281	1.9	3.4042
	6 ← 6	809 439.8640	2.0	2.9961
	8 ← 8	809 439.8866	2.0	3.9371
$6_{3,3} \leftarrow 6_{2,4}$	6 ← 6	814 218.0145	1.9	2.7678
	5 ← 5	814 218.1323	2.0	2.3894
	7 ← 7	814 218.1790	2.1	3.2829
$5_{3,2} \leftarrow 5_{2,3}$	4 ← 4	817 309.9877	2.1	1.7858
	5 ← 5	817 310.0061	2.0	2.1245
	6 ← 6	817 310.0685	2.2	2.6123
$4_{3,1} \leftarrow 4_{2,2}$	3 ← 3	819 127.8552	2.2	1.1784
	5 ← 5	819 127.9909	2.4	1.8963
	4 ← 4	819 128.0488	2.1	1.4586
$3_{3,0} \leftarrow 3_{2,1}$	2 ← 2	820 063.5048	2.4	0.5669
	4 ← 4	820 063.7514	2.5	1.0762
	3 ← 3	820 063.9805	2.2	0.7503
$3_{3,1} \leftarrow 3_{2,2}$	2 ← 2	820 699.5325	2.4	0.5666
	4 ← 4	820 699.8092	2.5	1.0757
	3 ← 3	820 700.1208	2.2	0.7499
$4_{3,2} \leftarrow 4_{2,3}$	3 ← 3	821 024.6294	2.2	1.1767
	5 ← 5	821 024.8065	2.3	1.8935
	4 ← 4	821 025.0144	2.1	1.4565
$5_{3,3} \leftarrow 5_{2,4}$	4 ← 4	821 697.1333	2.1	1.7798
	6 ← 6	821 697.2669	2.2	2.6036
	5 ← 5	821 697.4374	2.0	2.1174
$6_{3,4} \leftarrow 6_{2,5}$	5 ← 5	822 884.0631	1.9	2.3734
	7 ← 7	822 884.1739	2.1	3.2610
	6 ← 6	822 884.3381	1.9	2.7493
$7_{3,5} \leftarrow 7_{2,6}$	6 ← 6	824 775.5387	1.9	2.9600
	8 ← 8	824 775.6366	2.0	3.8896
	7 ← 7	824 775.8115	1.9	3.3631
$8_{3,6} \leftarrow 8_{2,7}$	7 ← 7	827 579.5682	1.9	3.5411
	9 ← 9	827 579.6584	2.0	4.5003
	8 ← 8	827 579.8547	1.9	3.9645
$13_{1,13} \leftarrow 12_{0,12}$	13 ← 12	831 306.1854	2.6	9.7131
	14 ← 13	831 306.5306	2.7	10.495
	12 ← 11	831 306.5563	2.6	8.9892
$9_{3,7} \leftarrow 9_{2,8}$	8 ← 8	831 516.3210	1.9	4.1167
	10 ← 10	831 516.4069	2.0	5.0974

Table 3. continued.

$J'_{K_a,K_c} \leftarrow J_{K_a,K_c}$	$F'_N \leftarrow F_N$	Calculated (MHz)	Uncertainty (kHz)	Line Strength
	$9 \leftarrow 9$	831 516.6315	1.9	4.5556
$6_{2,5} \leftarrow 5_{1,4}$	$6 \leftarrow 5$	836 673.8796	1.8	2.3260
	$7 \leftarrow 6$	836 674.9058	2.0	2.7605
	$5 \leftarrow 4$	836 675.0747	1.8	1.9575
$10_{3,8} \leftarrow 10_{2,9}$	$9 \leftarrow 9$	836 812.1056	2.0	4.6853
	$11 \leftarrow 11$	836 812.1891	2.0	5.6817
	$10 \leftarrow 10$	836 812.4469	2.0	5.1362
$5_{2,3} \leftarrow 4_{1,4}$	$4 \leftarrow 3$	843 259.6525	1.7	1.3911
	$6 \leftarrow 5$	843 260.0903	1.9	2.1137
	$5 \leftarrow 4$	843 261.4307	1.7	1.7170
$13_{1,12} \leftarrow 12_{1,11}$	$13 \leftarrow 12$	851 461.9892	2.7	12.809
	$14 \leftarrow 13$	851 462.0793	2.7	13.840
	$12 \leftarrow 11$	851 462.0801	2.7	11.855
$7_{2,6} \leftarrow 6_{1,5}$	$7 \leftarrow 6$	884 836.9203	1.9	2.6271
	$8 \leftarrow 7$	884 837.9572	2.1	3.0394
	$6 \leftarrow 5$	884 838.1045	1.9	2.2692
$6_{2,4} \leftarrow 5_{1,5}$	$5 \leftarrow 4$	924 782.5074	1.8	1.5009
	$7 \leftarrow 6$	924 782.8919	2.0	2.1167
	$6 \leftarrow 5$	924 784.3360	1.8	1.7835
$8_{2,7} \leftarrow 7_{1,6}$	$8 \leftarrow 7$	930 505.7424	2.1	2.9501
	$9 \leftarrow 8$	930 506.7810	2.2	3.3495
	$7 \leftarrow 6$	930 506.9131	2.0	2.5974
$9_{2,8} \leftarrow 8_{1,7}$	$9 \leftarrow 8$	973 791.7452	2.3	3.3007
	$10 \leftarrow 9$	973 792.7776	2.4	3.6937
	$8 \leftarrow 7$	973 792.8985	2.3	2.9488

Notes. [(a)] Transitions are labelled by the quantum numbers of upper and lower states: the rotational angular momentum J, its projections along the a-axis, K_a, and the c-axis, K_c, and the total angular momentum $F_N = J + I_N$.

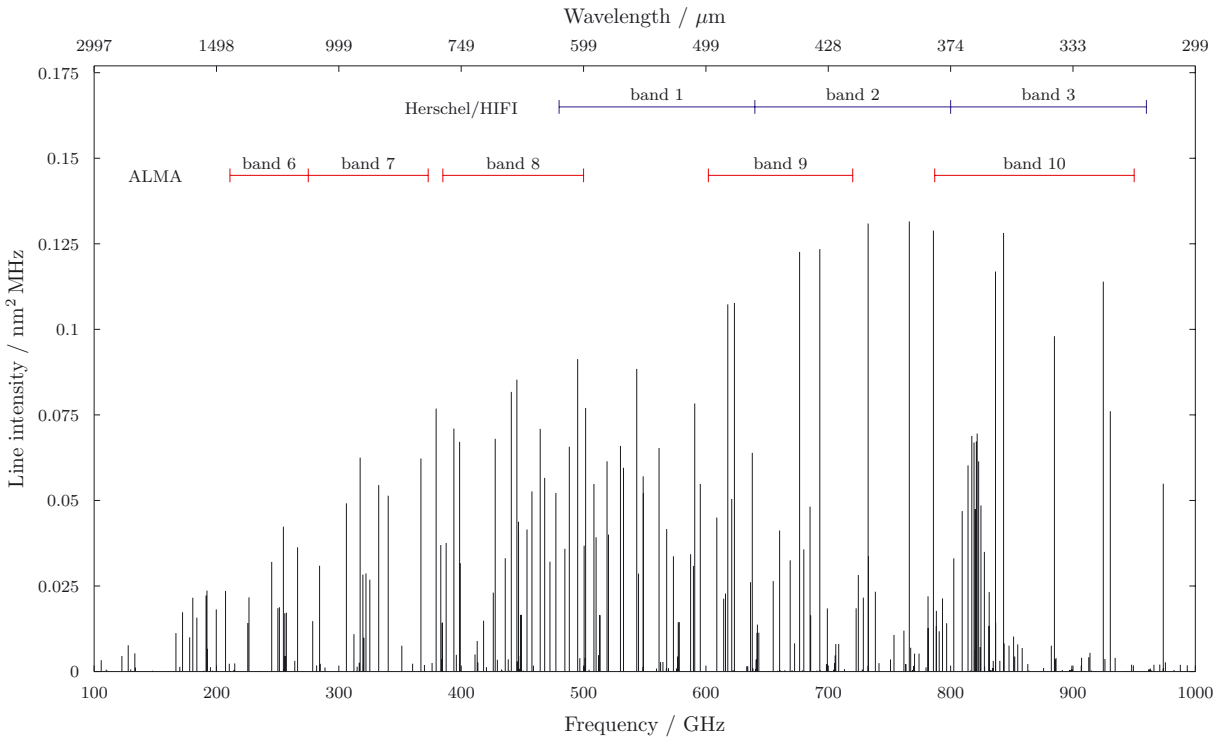

Fig. 2. Simulation of the rotational spectrum of CH_2NH. Intensities are computed at 50 K.

Acknowledgements. Financial support from MIUR (PRIN 2009 funds, project "Spettroscopia molecolare per la Ricerca Atmosferica e Astrochimica: Esperimento, Teoria ed Applicazioni") and from the University of Bologna (RFO funds) is gratefully acknowledged. L.B. gratefully acknowledges support from the Science and Technology Foundation (FCT, Portugal) through the Fellowship SFRH/BPD/62966/2009.

References

Allegrini, M., Johns, J. W. C., & McKellar, A. R. W. 1979, J. Chem. Phys., 70, 2829

Balucani, N., Bergeat, A., Cartechini, L., et al. 2009, J. Phys. Chem. A, 113, 11138

Belloche, A., Menten, K. M., Comito, C., et al. 2008, A&A, 482, 179
Bergin, E. A., Phillips, T. G., Comito, C., et al. 2010, A&A, 521, L20
Bizzocchi, L., & Degli Esposti, C. 2004, ApJ, 614, 518
Bizzocchi, L., Degli Esposti, C., & Dore, L. 2008, A&A, 492, 875
Costain, C. C. 1969, Can. J. Phys., 47, 2431
Danger, G., Borget, F., Chomat, M., et al. 2011, A&A, 535, A47
Dickens, J. E., Irvine, W. M., & DeVRries, C. H. 1997, ApJ, 479, 307
Dore, L. 2003, J. Mol. Spectr., 221, 93
Dore, L., Degli Esposti, C., Mazzavillani, A., & Cazzoli, G. 1999, Chem. Phys. Lett., 300, 489
Dore, L., Bizzocchi, L., Degli Esposti, C., & Gauss, J. 2010, J. Mol. Spectr., 263, 44
Godfrey, P. D., Brown, R. D., Robinson, B. J., & Sinclair, M. W. 1973, Astrophys. Lett., 113, 119
Halonen, L., & Duxbury, G. 1985, J. Chem. Phys., 83, 2078
Hamada, Y., Hashiguchi, K., & Tsuboi, M. 1984, J. Mol. Spectr., 105, 70
Johnson, D. R., & Lovas, F. J. 1972, Chem. Phys. Lett., 15, 65
Martín, S., Mauersberger, R., Martín-Pintado, J., Henkel, C., & García-Burillo, S. 2006, ApJS, 164, 450
Muller, S., Beelen, A., Guélin, M., et al. 2011, A&A, 535, A103
Pearson, R., & Lovas, F. J. 1977, J. Chem. Phys., 66, 4149
Pickett, H. M. 1991, J. Mol. Spectr., 148, 371
Qin, S.-L., Wu, Y., Huang, M., et al. 2010, ApJ, 711, 399
Redondoa, P., Pauzatb, F., & Ellinger, Y. 2006, Planet Space Sci., 54, 181
Salter, C. J., Ghosh, T., Catinella, B., et al. 2008, Astron. J., 136, 389
Schilke, P., Benford, D. J., Hunter, T. R., Lis, D. C., & Phillips, T. G. 2001, ApJS, 132, 281
Tenenbaum, E. D., Dodd, J. L., Milam, S. N., Woolf, N. J., & Ziurys, L. M. 2010, ApJ, 720, L102
Turner, B. E. 1991, ApJS, 76, 617
Turner, B. E., Terzieva, R., & Herbst, E. 1999, ApJ, 518, 699
Vuitton, V., Yelle, R. V., & McEwan, M. J. 2007, Icarus, 191, 722
Watson, J. K. G. 1977, Aspects of quartic and sextic centrifugal effects on rotational energy levels, Vibrational Spectra and Structure (Amsterdam: Elsevier), 6, 1
White, G. J., Araki, M., Greaves, J. S., Ohishi, M., & Higginbottom, N. S. 2003, A&A, 407, 589
Winton, R., & Gordy, W. 1970, Phys. Lett. A, 32, 219
Yamada, K. M. T., Degli Esposti, C., Botschwina, P., et al. 2004, A&A, 425, 767